13. The steps in the procedure are as follows:

1. Determine the superstructure for the multipurpose plant design problem.

2. Delete any products that appear in the same periods as the first product from consideration for constraints involving this first product.

3. From the subset of remaining products, consider all combinations of this subset that do not share a common period. Use these particular combinations with the first product to list its horizon constraints. If this subset of products is the empty set, consider the processing time of the first product to be less than the total available time as the only possible contraint in this step.

4. Omit the first product from analysis. Repeat steps 2–4 with each subsequent product until all products have been considered.

5. Delete redundant constraints.

6. Check the final set of horizon constraints to see that at least one constraint contains all the time periods. If this condition is met, the merged formulation can be used. If none of the new horizon constraints has all of the periods, a nontypical case, then a partial merging of the constraints can be used, as explained in the partially merged formulation.

From the example in Figure 3 the resulting tree search is shown in Figure 14 with "X" representing the exclusion of the rest of the branch. In the branch ABC, products A and B do not have any time periods in common, but C is contained in period 1 with product A. Thus, the branch AB is a viable constraint.

$$T_A + T_B \leq H \quad \text{(A1)}$$

The other two horizon constraints are shown in branches AD and BC.

$$T_A + T_D \leq H \quad \text{(A2)}$$

$$T_B + T_C \leq H \quad \text{(A3)}$$

The constraint from branch C, $T_C \leq H$, is deleted since it is redundant due to constraint (A3). Also, the constraint from branch D, $T_D \leq H$, is redundant because of constraint (A2).

Literature Cited

Garfinkel, R. S.; Nemhauser, G. L. *Integer Programming*; Wiley: New York, 1972.

Grossmann, I. E.; Sargent, R. W. H. *Ind. Eng. Chem. Process Des. Dev.* **1979**, *18*, 343–348.

Imai, M.; Nishida, N. *Ind. Eng. Chem. Process Des. Dev.* **1984**, *23*, 845–847.

Klossner, J.; Rippin, D. W. T. Paper presented the AIChE Annual Meeting, San Francisco, Nov 1984.

Murtagh, B. A.; Saunders, M. A. MINOS/AUGMENTED User's Manual. Technical Report SOL 80-14, Stanford University Systems Optimization Laboratory, June 1980.

Sparrow, R. G.; Forder, G. J.; Rippin, D. W. T. *Ind. Eng. Chem. Process Des. Dev.* **1975**, *14*, 197.

Suhami, I.; Mah, R. S. H. *Ind. Eng. Chem. Process Des. Dev.* **1982**, *21*, 94–100.

Vaselenak, J. A. Ph.D. Dissertation, Carnegie-Mellon University, Pittsburgh, PA, 1985.

Received for review October 4, 1985
Revised manuscript received May 27, 1986
Accepted June 13, 1986

Aqueous-Phase Oxidation: The Intrinsic Kinetics of Single Organic Compounds

Richard S. Willms,[†] Anne M. Balinsky,[‡] Danny D. Reible, David M. Wetzel, and Douglas P. Harrison*

Department of Chemical Engineering, Louisiana State University, Baton Rouge, Louisiana 70803

The aqueous-phase oxidation of *m*-xylene and phenol has been studied in a batch autoclave reactor. Both reactions were characterized by an induction period during which little of the organic was oxidized, followed by a rapid reaction phase during which most of the organic was destroyed. The distribution of organic between vapor and liquid and interphase transfer caused by liquid-phase reaction and sampling were considered in the analysis of the data. Over the range of concentrations studied, the length of the induction period is independent of the organic concentration and inversely proportional to the dissolved oxygen concentration. During the rapid reaction phase, the oxidation kinetics are first order in organic and half order in dissolved oxygen. Activation energies for *m*-xylene and phenol were found to be 103 and 94 kJ/g-mol during the induction period and 89.5 and 112 kJ/g-mol during the rapid reaction phase.

Organic compounds in aqueous solution are known to oxidize at temperatures and pressures of approximately 473 K and 13.8 MPa of air. This concept forms the basis for the Wetox process for wastewater treatment, currently used in approximately 200 installations worldwide (Canney et al., 1984). Applications include municipal waste treatment and effluent treatment from the pulp and paper and chemical-processing industries.

In spite of this rather extensive commercial application, fundamental information on oxidation kinetics—reaction orders and activation energies—and reaction mechanisms is extremely meager and often contradictory. For example, a range of values for the activation energy for the uncatalyzed oxidation of phenol from 20.5 kJ/g-mol (Helling et al., 1981) to 107 kJ/g-mol (Shibaeva et al., 1969) has been reported. The reaction order with respect to oxygen in the rapid reaction phase has been reported to be one-half (Sadana and Katzer, 1974) and one (Shibaeva et al., 1969). One study (Pujol et al., 1980) reports that the activation energy for the oxidation of pulping liquor

[†] Present address: Los Alamos National Laboratory, Los Alamos, NM 87545.

[‡] Present address: 14 Wilkinson Road, Randolph, NJ 07869.

0888-5885/87/2626-0148$01.50/0

Table I. Run Conditions and Model Results for *m*-Xylene, Phenol, and Tetrachloroethylene

T, K	P, MPa	M_0, kg × 10^3	t_s, s × 10^{-3}	k', 1/s × 10^3	$[O_2]$, kg/L × 10^3	k, (1/s)(L/kg)$^{0.5}$
			m-Xylene			
473	13.8	0.053	7.92	0.448	0.999	0.0142
473	13.8	0.056	8.34	0.411	0.999	0.0130
473	13.8	0.083	10.5	0.645	0.999	0.0204
473	13.8	0.090	19.1	0.435	0.999	0.0138
473	13.8	0.092	19.9	0.418	0.999	0.0132
473	13.8	0.103	9.41	0.592	0.999	0.0187
473	13.8	0.106	6.93	0.507	0.999	0.0160
473	13.8	0.107	7.68	0.466	0.999	0.0147
473	13.8	0.162	8.22	0.475	0.999	0.0150
473	13.8	0.162	9.72	0.421	0.999	0.0133
473	13.8	0.163	7.32	0.482	0.999	0.0152
473	14.5	0.108	16.6	0.436	1.05	0.0134
498	6.89	0.109	10.8	1.19	0.436	0.0569
498	6.89	0.115	9.40	1.22	0.436	0.0585
498	10.3	0.091	3.58	1.59	0.782	0.0568
498	10.3	0.104	3.36	1.67	0.782	0.0596
498	13.8	0.094	3.22	1.80	1.13	0.0537
498	13.8	0.104	9.13[a]	1.80	1.13	0.0535
513	6.89	0.089	2.18	1.72	0.409	0.0849
513	6.89	0.090	3.88	1.56	0.409	0.0769
513	10.3	0.090	1.36	2.10	0.807	0.0740
513	10.3	0.107	1.22	2.17	0.807	0.0763
			Phenol			
403	13.8	0.110	19.3	0.290	0.730	0.0107
415	13.8	0.120	9.21	0.833	0.761	0.0302
427	13.8	0.117	4.45	2.15	0.799	0.0761
439	13.8	0.110	1.59	4.80	0.844	0.165
451	13.8	0.115			0.895	
473	13.8	0.110			0.999	
			Tetrachloroethylene			
498	17.2	0.068	0	0.00275	1.47	0.0000717
548	13.8	0.103	0	0.0222	1.33	0.000608

[a] Datum point rejected on the basis of statistical tests.

changes abruptly from 13.4 to 135 kJ/g-mol at 563 K. Perhaps the most common point of agreement is that the reaction order with respect to the parent organic compound is one, although there is an indication of a shift in reaction order at very low organic concentrations (Chowdhury and Ross, 1975; Baillod and Faith, 1983).

There are a number of apparent reasons for this lack of agreement. First, the problem of sampling and analyzing dilute aqueous solutions at these conditions is not easy. Second, phase equilibrium effects with the possible distribution of organic between vapor and liquid have not always been recognized. Third, apparent errors in the experimental procedure and method of data analysis, particularly with respect to oxygen, may be cited.

In this study, a "sampled batch" reactor has been used to investigate the oxidation kinetics of *m*-xylene, phenol, and tetrachloroethylene. Only the rate of destruction of the parent organic has been studied. No attempt was made to monitor the appearance/disappearance of partially oxidized intermediates, as the additional analytical complications would have severely limited the amount of data which could be collected during a single run. The data have been analyzed by using a model (Willms et al., 1985) which accounts for phase equilibrium of moderately volatile species as well as the change in liquid and vapor volumes which accompany sampling.

Experimental Section

Figure 1 shows the experimental apparatus. Since the details have been described previously (Willms et al., 1985), only key features will be repeated. The reaction vessel was a 1-L stainless steel autoclave equipped with a six-bladed, magnetically driven turbine agitator. A Valco sampling valve was used to inject 1-μL samples directly into a gas chromatograph. The valve and sampling line were heated and operated at reactor pressure to prevent composition changes. Five milliliters of reacting liquid was flushed through the sampling valve just prior to injection to ensure that the sample analyzed was representative of the reaction mixture at that time.

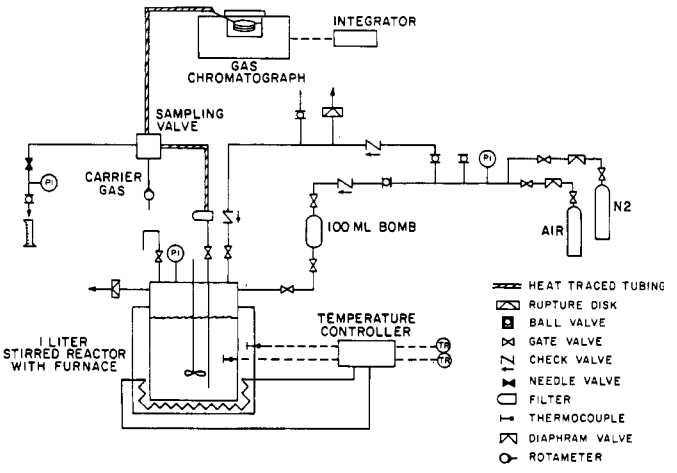

Figure 1. Experimental apparatus.

The reactor was first charged with 700 mL of distilled water, pressurized with air, and heated to reaction temperature. Approximately 10^{-4} kg of organic (the exact quantity is shown in Table I) was then flushed into the reactor by using 80 mL of distilled water. By use of this procedure, the water was largely presaturated with oxygen, the time at which the reaction began was precisely defined, and initial temperature and pressure upsets were minimized. During the course of the reaction, samples were periodically injected into the gas chromatograph.

A Perkin-Elmer 990 gas chromatograph equipped with dual-flame ionization detectors was used for analysis. Response data were recorded and processed on a Hewlett-Packard Model 3390A integrator. For phenol analysis, a 6-ft. by 2-mm-i.d. glass column packed with 4% OV-17 on 80/100-mesh Gas Chrom Q was used. Tetrachloroethylene analysis used a glass column of the same size packed with 5% SP-1200 and 1.75% Bentone 34 on 100/120-mesh Supelcoport. Both of these columns were used in *m*-xylene experiments. The column was operated isothermally in all cases with T = 383 K for phenol, T = 353 K for tetrachloroethylene, and T = 383 and 363 K for *m*-xylene using the OV-17 and SP-1200 columns, respectively. Approximate elution times for the compounds were 100 s for phenol, 130 s for tetrachloroethylene, and 40 and 140 s for *m*-xylene on OV-17 and SP-1200, respectively.

Model

Aqueous-phase oxidation generally proceeds according to a free-radical mechanism characterized by an induction period during which little of the parent organic is oxidized followed by a rapid reaction period during which the majority of the organic is consumed. The length of the induction period is determined by the time required for the free-radical concentration to reach a minimum critical value. The mathematical model (Willms et al., 1985) is based upon such a reaction system.

During the induction period, each liquid sample withdrawn alters the liquid and vapor volumes, resulting in redistribution of the remaining organic between the vapor and liquid. Vapor–liquid equilibrium is assumed to be reestablished instantaneously after each sample. While the concentration change associated with a single sample is small, cumulative sampling during an extended run can have a significant effect on concentration. During the rapid reaction phase, depletion of organic from the liquid phase upsets the phase equilibrium and causes organic from the vapor phase to be transferred to the liquid. The mass-transfer rate is assumed to be sufficiently fast so that a pseudoequilibrium is maintained at all times. The effect of sampling is the same during the induction and rapid reaction phases.

Further assumptions in the model are that phase equilibrium can be described by Henry's law, the vapor phase is ideal, and no reaction occurs in the vapor phase. Finally, the model assumes the intrinsic kinetics to be first order in organic and nth order in dissolved oxygen. The dissolved oxygen is assumed to be always present in great excess, thereby simplifying the kinetics to pseudo first order. Separate tests at different oxygen pressures are necessary to identify the order with respect to oxygen.

The step function change in concentration associated with sampling is given by

$$[\mathrm{RH}]_a = \frac{\phi_0 - V_S}{\phi}[\mathrm{RH}]_b \qquad (1)$$

where ϕ is defined as

$$\phi = V_L + \frac{HM(V_T - V_L)}{RT\rho} \qquad (2)$$

Once the rapid reaction phase begins, the concentration change which occurs in the time interval between samples is

$$[\mathrm{RH}]_t = [\mathrm{RH}]_a \exp\left[-\frac{k'V_L}{\phi}(t - t_a)\right] \qquad (3)$$

During the induction period, eq 1 is applied each time a sample is taken; the result is an instantaneous change in liquid concentration. Once the rapid reaction phase begins, the liquid-phase concentration is diminished continuously due to reaction (eq 3) and discontinuously and instantaneously due to sampling (eq 1).

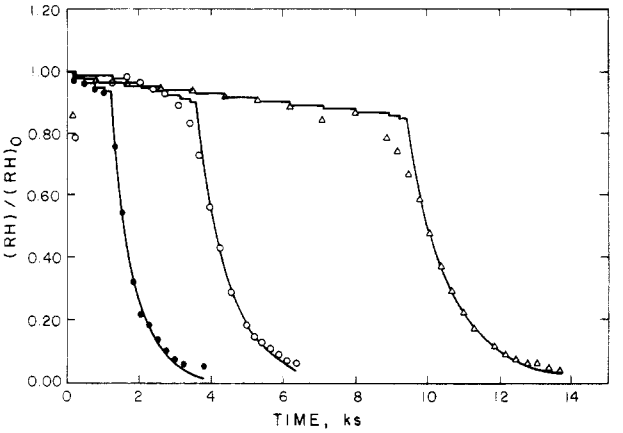

Figure 2. Experimental data and model curves for *m*-xylene: (△) 498 K, 6.89 MPa; (○) 498 K, 10.3 MPa; (●) 513 K, 10.3 MPa.

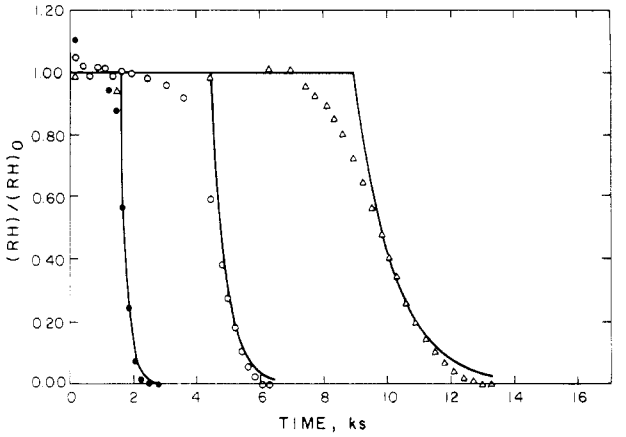

Figure 3. Experimental data and model curves for phenol: (△) 415 K, 13.8 MPa; (○) 427 K, 13.8 MPa; (●) 439 K, 13.8 MPa.

It is useful to observe that all vapor–liquid equilibrium effects during reaction are accounted for in the ratio V_L/ϕ. If Henry's constant is zero, all organic remains in the liquid phase, the ratio is unity, and eq 3 reduces to the familiar integrated form of the first-order rate equation. In contrast, an infinitely large value of H forces the ratio to zero, and eq 3 indicates no change in concentration with time. All organic is in the vapor phase so that no liquid-phase reaction is possible.

The model requires only liquid-phase concentration measurements, eliminating the need for vapor-phase sampling and analysis. A complete concentration history of liquid-phase oxidation reactions which follow the assumptions stated in the model development is thus available.

Experimental Results

Table I summarizes the reaction temperature, pressure, and initial mass of organic injected for each of the experimental runs. Also included are the kinetic parameters determined from the model analysis. Typical concentration–time experimental results for *m*-xylene, phenol, and tetrachloroethylene are summarized in Figures 2, 3, and 4, respectively. For the moment, let us concentrate upon the discrete points which designate the experimental results. The solid lines which represent the results of the mathematical model will be discussed in the following section.

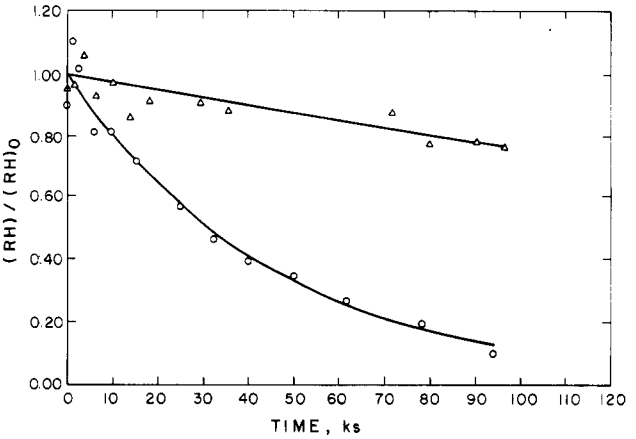

Figure 4. Experimental data and model curves for tetrachloroethylene: (△) 498 K, 17.2 MPa; (○) 548 K, 13.8 MPa.

In both the *m*-xylene and phenol reactions, the induction and rapid reaction phases are clearly visible. No induction period was observed with the tetrachloroethylene tests. In each case there is considerable experimental scatter associated with the first two or three data points. This is attributed to the time required to dissolve the organic and establish vapor–liquid equilibrium.

The *m*-xylene results in Figure 2 show clearly that the length of the induction period decreases with increasing pressure and temperature. Although not so obvious visually, the oxidation rate during the rapid reaction phase increases with both temperature and pressure.

The results of runs at 473 K were consistent with the higher temperature results. Induction times were longer, and oxidation rates were slower. The data scatter, particularly with respect to the length of the induction time was increased. This is due to the fact that 473 K is approximately the minimum temperature at which the *m*-xylene oxidation reaction can be self-initiated. In an exploratory test at 463 K, the induction period was longer than 2×10^4 s, and the rapid reaction phase was never reached.

Phenol oxidation results shown in Figure 3 are qualitatively quite similar to the *m*-xylene results. All phenol runs were made at 13.8 MPa of air, so the only effect shown is that of temperature. The data scatter in the first few samples is less severe, presumably because of the greater solubility and lower volatility of phenol. Both the induction period and the rapid reaction phase are clearly visible. Phenol, however, is considerably more reactive than *m*-xylene, in that comparable reaction rates can be achieved at the lower temperatures (415–439 K) shown in the figure.

The results of two oxidation tests using tetrachloroethylene are shown in Figure 4. No induction period is visible, but even at these more severe temperatures the reaction is much slower, with the reaction times increased by a factor of approximately 10. The modeling analysis showed that the concentration–time dependence is exponential as expected for a first-order reaction. Because of the extreme reaction conditions and slow rates associated with tetrachloroethylene, this compound was not studied in greater detail. Results are included here primarily to establish that not all compounds exhibit the characteristic induction period followed by the rapid reaction phase.

Application of the Model

Three of the basic assumptions made in deriving the phase equilibrium-reaction model require further justification for the systems studied. These concern the ideality of the gas phase, the absence of mass-transfer resistances between vapor and liquid, and the fact that dissolved oxygen is in such excess that its concentration can be considered constant throughout a run.

Gas-phase ideality at the experimental conditions was easily shown by comparing ideal gas calculations to those of the Redlich–Kwong equation of state over the temperature and pressure ranges of interest. Differences were quite small.

The mass-transfer question was addressed as follows. By equating the rate of oxygen transfer from the gas to liquid phase to the rate of oxygen consumption by reaction in the liquid phase, the following equation results which relates the actual dissolved oxygen concentration to the equilibrium value

$$\frac{[O_2]}{[O_2]^*} = 1 - \frac{V_L S k' [RH]}{k_L a [O_2]^*} \tag{4}$$

Mass-transfer coefficients were estimated by using generalized correlations presented by Barona (1979). The stoichiometric coefficient, S, was based upon total oxidation of the parent organic to CO_2 and H_2O (S = 10.5 for xylene). By use of known values of $[RH]_0$ and values of k' determined by model analysis (reported in Table I), values of $[O_2]/[O_2]^*$ were calculated. In the worst case for *m*-xylene at 513 K and 10.3 MPa, the dissolved oxygen concentration could be reduced from its equilibrium value by as much as 10%. However, since oxidation does not proceed immediately to CO_2 and H_2O, and since this maximum rate exists only instantaneously, the acutal oxygen depletion is always less than the 10% value. Similar arguments hold for phenol. Although the k' values for phenol are higher, the stoichiometric coefficient is smaller and the final conclusion is the same. Thus, the assumption of no mass-transfer limitation is valid.

Because the water was effectively saturated initially, it is possible to calculate the total amount of oxygen in solution at the beginning of the reaction by using the Henry's constant values for oxygen in water presented by Himmelblau (1960). The ratios of the dissolved oxygen at the beginning of the reaction to the oxygen required for complete oxidation (to CO_2 and H_2O) with each of the parent organics over the range of experimental conditions were then calculated with the following results: *m*-xylene, 1.03–2.76; phenol, 2.39–3.53; and tetrachloroethylene, 35.4–52.5. Therefore, the large concentration of dissolved oxygen present initially, coupled with the rapid mass transfer previously shown, justifies the assumption of constant oxygen concentration and the use of pseudo-first-order kinetics.

The Henry's law constants for the parent organic species at the temperatures and pressures of interest are the final information needed to apply the model. For a sparingly soluble compound, Henry's law holds over the entire range of solubility. At equilibrium solubility, x^*, the compound will exert its full, pure component vapor pressure, p^*. Thus,

$$H^R = p^*/x^* \tag{5}$$

Vapor pressures for *m*-xylene as a function of temperature were obtained from Vargaftik (1983). Solubilities as a function of temperature at the vapor pressure of water were obtained from the American Petroleum Institute Technical Data Book (1983), and values of H^R were computed. The calculated values are those of *m*-xylene in water, and no attempt was made to consider any effect of the trace species present. Since experiments were conducted at pressures above the vapor pressure of water, the

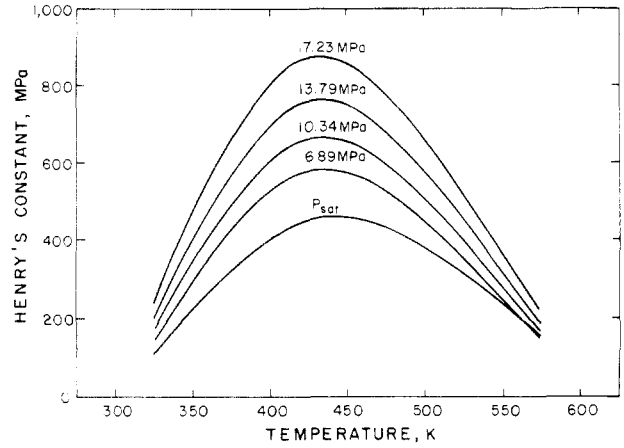

Figure 5. Calculated Henry's law constants for *m*-xylene.

Poynting correction (Heidman et al., 1985) was used to correct the H^R values to the actual pressure:

$$H = H^R \exp\left[\frac{M(P - p^R)}{\rho RT}\right] \quad (6)$$

Results of these calculations are presented in Figure 5. Experimental conditions covered the ranges of 473–513 K and 6.89–17.2 MPa. At these conditions, H increases with increasing pressure but decreases with increasing temperature. At a typical value of H = 600 MPa, approximately 30% of the *m*-xylene would be present in the vapor phase.

Because phenol is infinitely soluble in water at temperatures above 341 K and because its vapor pressure is less than that of *m*-xylene, the value of H for phenol was taken to be zero. The implication is that all phenol remains in the liquid phase, negating the requirement of phase-transfer calculations. Solubility data at the temperatures of interest could not be located for tetrachloroethylene. On the basis of the ambient temperature solubility and vapor pressure, one would expect H for tetrachloroethylene to be less than that for *m*-xylene but greater than zero. The value was taken to be zero, since the tetrachloroethylene portion of the study was much less important than the *m*-xylene and phenol phases, and the required data were not available.

The model was then applied to each of the experimental runs with the typical match of experiment and model shown in Figures 2–4. The time corresponding to the end of the induction period, t_s, and the pseudo-first-order rate constant, k', were the regression values. Note that the experimental data show a gradual transition from the induction to the rapid reaction phases. The model assumes an abrupt transition and, therefore, does not match the data in this area. Because of this transition, care had to be exercised in choosing experimental points which were clearly in the rapid reaction phase for the regression analysis.

The assumed first-order kinetics in organic fits the data quite well during most of the rapid reaction period. Near the end of the reaction, the experimental concentrations decrease more slowly than the model predicts. This apparent change in reaction order at low concentrations has been reported by others including Chowdhury and Ross (1975) and Baillod and Faith (1983). We attribute this phenomenon to autoinhibition caused by the buildup of partially oxidized intermediates which compete with the parent organic for free radicals.

Calculated values of t_s and k' for each of the runs are summarized in Table I. The blanks in the phenol group

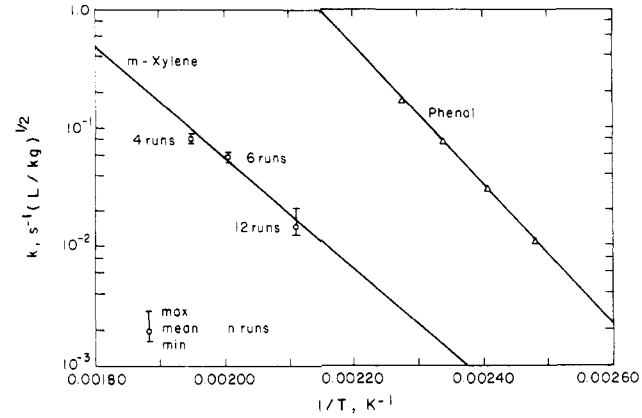

Figure 6. Rapid reaction-phase Arrhenius analysis for *m*-xylene and phenol.

Table II. Summary of Kinetic Parameters for Oxidation of *m*-Xylene and Phenol

	induction phase: $t_s = [R^\cdot]_s/A_i[O_2]\exp(E_i/RT)$	
	$[R^\cdot]_s/A_i$, kg s/L	E_i, kJ/g-mol[a]
m-xylene	4.50×10^{-11}	103 ± 20
phenol	9.42×10^{-12}	94 ± 31
	rapid reaction phase: $d[RH]/dt = -A_r[O_2]^{1/2}[RH]\exp(-E_r/RT)$	
	A_r, $L^{1/2}/(s\ kg^{1/2})$	E_r, kJ/g-mol[a]
m-xylene	1.19×10^8	89.5 ± 8.6
phenol	3.65×10^{12}	112 ± 13

[a] All confidence limits are at the 95% level.

corresponding to the two highest temperatures indicate that the reaction was so fast at these conditions that insufficient data could be acquired to permit meaningful regression.

Further analysis of the data (to be discussed) showed that during the rapid reaction phase the rate was half order in oxygen, in agreement with the reports of Sadana and Katzer (1974) and Day et al. (1973), but in contrast to the first-order oxygen dependence reported by others. The intrinsic rate constant, k, shown in the last column of Table I was thus obtained by dividing k' by $[O_2]^{1/2}$.

The temperature dependence of k for both *m*-xylene and phenol has been analyzed according to the Arrhenius equation with results shown in Figure 6. The spread in the *m*-xylene results at a particular temperature shows no correlation with pressure. In contrast, when k was calculated by using other reaction orders for oxygen, for example, first order, the linearity of the resulting Arrhenius plot was not as good, and there was an apparent pressure dependence in the data spread at a fixed temperature. Hence, the order with respect to oxygen was determined to be one-half.

From the linear least-squares lines through the data, the activation energies and frequency factors shown in Table II were determined. Confidence limits on the activation energies are at the 95% level. It is interesting to note that the phenol activation energy agrees very well with the value of 107 kJ/g-mol reported by Shibaeva et al. (1969) and that both are well above the values reported by others. For example, Baillod and Faith (1983) report E = 33.1 kJ/g-mol, Helling et al. (1981) report E = 20.5 kJ/g-mol, and Pruden and Le (1976) report E = 45.3 kJ/g-mol. No previous work on *m*-xylene is available, so comparisons are not possible. However, the value of 89.5 kJ/g-mol is certainly reasonable and lends added weight to the arguments that phase-transfer resistances are unimportant.

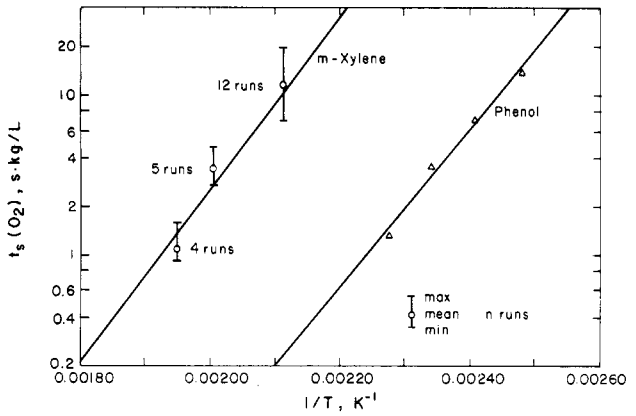

Figure 7. Induction-phase Arrhenius analysis for *m*-xylene and phenol.

It was found that the length of the induction period could also be correlated by using an Arrhenius analysis developed from pseudomechanistic arguments. The initiation reaction which controls the rate of formation of radicals during the induction period is believed to be first order in dissolved oxygen concentration and zero order in organic. Hence,

$$\frac{d[R^\bullet]}{dt} = k_i[RH]^0[O_2]^1 \tag{7}$$

During the induction period both [RH] and $[O_2]$ are essentially constant. Therefore, integrating and substituting the Arrhenius equation produces

$$[R^\bullet] = A_i \exp(-E_i/RT)[O_2]_0 t \tag{8}$$

Next, we postulate that some critical concentration of free radicals, $[R^\bullet]_s$, corresponds to the onset of the rapid reaction phase at $t = t_s$. This concentration is presumed to be independent of the temperature over the range of temperatures studied. Therefore, letting $[R^\bullet] = [R^\bullet]_s$ and $t = t_s$ and rearranging eq 8 yield

$$\ln (t_s[O_2]_0) = \ln ([R^\bullet]_s/A_i) + (E_i/RT) \tag{9}$$

A plot of $\ln (t_s[O_2]_0)$ vs. $1/T$ should yield a straight line with a slope of E_i/R. Although $[O_2]$ is constant for a given run, it changes from run to run as the pressure is altered. Such a plot is shown in Figure 7. Arrhenius parameters obtained by regression analysis of the Figure 7 data are summarized in Table II. Again, confidence limits on the reported activation energies are at the 95% level. No previous analysis of this type could be found in the literature for aqueous-phase oxidations. However, Denisova and Denisov (1969) report an activation energy for the initiation reaction of *o*-xylene in benzene of 130 kJ/g-mol, in reasonable agreement with our value of 103 ± 20 kJ/g-mol.

The first-order oxygen dependence in the initiation reaction was determined by constructing the Arrhenius plot assuming various orders as was done in the Arrhenius analysis of the rapid reaction phase. Orders other than one increased the scatter in the data and showed a visible pressure dependence. The zero-order dependence in organic concentration was determined by noting no significant change in t_s for changes in $[RH]_0$. At 473 K and 13.8 MPa, the two runs at low initial *m*-xylene concentration ($m_0 = 5.4 \times 10^{-5}$ kg) produced an average t_s of 8130 s; three runs in which the initial concentration was increased by a factor of 3 ($m_0 = 16.2 \times 10^{-5}$ kg) gave an average t_s of 8420 s.

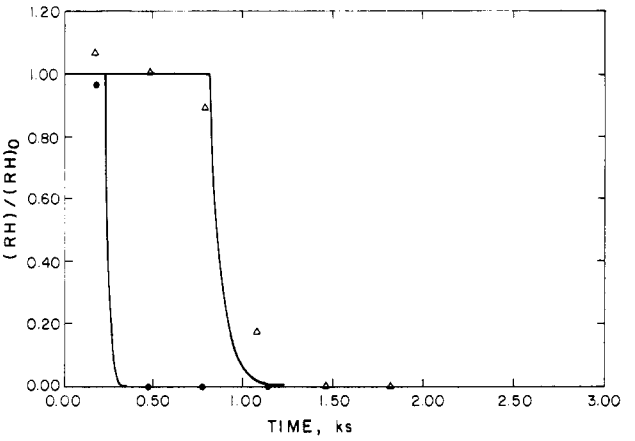

Figure 8. Experimental data and extrapolated model curves for phenol: (△) 451 K, 13.8 MPa; (●) 473 K, 13.8 MPa.

It was previously noted that the oxidation rate of phenol at the two higher temperatures, 451 and 473 K, was too fast to allow sufficient data to be acquired for meaningful regression analysis. It was possible, however, to extrapolate the Arrhenius parameters determined at the lower temperatures and predict the behavior at both of the higher temperatures. This result is shown in Figure 8. It is obvious that the model is in very good agreement with the limited number of experimental points during both the induction and rapid reaction phases. For example, at 473 K the first sample taken at 180 s showed no phenol depletion; the second sample at 480 s (and subsequent samples) indicated complete oxidation. The extrapolated model parameters give $t_s = 245$ s and predict the phenol to be depleted after 332 s, both in total agreement with the experimental data.

Summary

Experimental results have shown the aqueous-phase oxidation reactions of *m*-xylene and phenol at temperatures between 300 and 500 K, and pressures between 7 and 14 MPa are characterized by an induction period during which no change in the organic concentration can be detected, followed by a rapid reaction period. Over a threefold change in *m*-xylene concentration, no change in the length of the induction period was observed; however, the induction time was inversely proportional to the dissolved oxygen concentration. Activation energies during the induction phase were 103 ± 20 kJ/g-mol for *m*-xylene and 94 ± 31 kJ/g-mol for phenol.

During the rapid reaction period, the kinetics were first order in organic and half order in oxygen, with activation energies of 89.5 ± 8.6 and 112 ± 13 kJ/g-mol for *m*-xylene and phenol.

Limited experiments with the hydrogen-free compound tetrachloroethylene showed a lack of an apparent induction period and much more refractory behavior during the reaction.

Acknowledgment

This project has been supported, in part, with funds from the US Environmental Protection Agency under Contract 68-03-3014. The content of this paper has not been subjected to the Agency's required peer and policy review and therefore does not necessarily reflect the official views or policies of the US Environmental Protection Agency. Mention of trade names, commercial products, or organizations does not constitute endorsement or recommendation for use by the US government, Rockwell International, or Louisiana State University.

Nomenclature

A = frequency factor in the Arrhenius equation, units vary
E = activation energy in the Arrhenius equation, kJ/g-mol
H = Henry's law constant, MPa
k = intrinsic rate constant, units vary
k' = pseudo-first-order rate constant, s^{-1}
k_La = volumetric mass-transfer coefficient, L/s
m = mass of organic in reactor, kg
M = molecular weight of organic
$[O_2]$ = concentration of dissolved oxygen, kg/L
p = vapor pressure, MPa
P = reactor pressure, MPa
R = gas constant, MPa L/(kmol K) or J/(g-mol K)
[RH] = concentration of organic in solution, kg/L
$[R^\bullet]$ = concentration of free radicals in solution, L^{-1}
S = stoichiometric coefficient, dimensionless
t = time, s
T = temperature, K

Greek Symbols

ρ = liquid density, kg/L
ϕ = parameter defined by eq 2

Subscripts

O = initial conditions
a = just after sample is withdrawn
b = just before sample is withdrawn
i = induction phase
L = liquid
r = rapid reaction phase
s = start of the rapid reaction phase, end of the induction phase
T = total
t = at time t

Superscripts

* = at equilibrium
R = reference conditions (vapor pressure of water at T)

Registry No. O_2, 7782-44-7; *m*-xylene, 108-38-3; phenol, 108-95-2.

Literature Cited

American Petroleum Institute Technical Data Book, 4th ed.; American Petroleum Institute: Washington, DC, 1983.
Baillod, C. R.; Faith, B. M. 1983; Report EPA-600/S2-83-060, US Government Printing Office, Washington, DC.
Barona, N. *Hydrocarbon Process.* **1979**(July), 179.
Canney, P. J.; Dietrich, M. J.; Randall, T. L. Presented at the AIChE National Meeting, Philadelphia, 1984; Paper 41b.
Chowdhury, A. K.; Ross, L. W. *AIChE Symp. Ser.* **1975**, *71* (*151*), 46.
Day, D. C.; Hudgins, R. R.; Silveston, P. L. *Can. J. Chem. Eng.* **1973**, *51*, 733.
Denisova, L. N.; Denisov, E. T. *Kinet. Katal.* **1969**, *10*, 1244.
Heidman, J. L.; Tsonopoulos, C.; Brady, C. J.; Wilson, G. M. *AIChE J.* **1985**, *31*, 376.
Helling, R. K.; Strobel, M. K.; Torres, R. J. DOE Report, 1981; Union Carbide, Contract W-7405-ENG-26.
Himmelblau, D. M. *J. Chem. Eng. Data* **1960**, *5*, 10.
Pruden, B. B., and Le, H. *Can. J. Chem. Eng.* **1976**, *54*, 319.
Pujol, C. B.; Talayrach, B.; Besombes-Vailhe, J. *Water Res.* (*Fr.*) **1980**, *14*, 1055.
Sadana, A.; Katzer, J. R. *Ind. Eng. Chem. Fundam.* **1974**, *13*, 127.
Shibaeva, L. V.; Metelitsa, D. I.; Denisov, E. T. *Kinet. Catal.* **1969**, *10*, 832.
Vargaftik, N. B. *Handbook of Physical Properties of Liquids and Gases, Pure Substances and Mixtures*, 2nd ed.; Hemisphere: Washington, DC, 1983; p 351.
Willms, R. S.; Balinsky, A. M.; Reible, D. D.; Wetzel, D. M.; Harrison, D. P. *Env. Prog.* **1985**, *4*, 131.

Received for review December 3, 1985
Revised manuscript received May 27, 1986
Accepted June 13, 1986